creative commons
COMMONS DEED

저작자표시-비영리-변경금지 2.0 대한민국

이용자는 아래의 조건을 따르는 경우에 한하여 자유롭게

- 이 저작물을 복제, 배포, 전송, 전시, 공연 및 방송할 수 있습니다.

다음과 같은 조건을 따라야 합니다:

저작자표시. 귀하는 원저작자를 표시하여야 합니다.

비영리. 귀하는 이 저작물을 영리 목적으로 이용할 수 없습니다.

변경금지. 귀하는 이 저작물을 개작, 변형 또는 가공할 수 없습니다.

- 귀하는, 이 저작물의 재이용이나 배포의 경우, 이 저작물에 적용된 이용허락조건을 명확하게 나타내어야 합니다.
- 저작권자로부터 별도의 허가를 받으면 이러한 조건들은 적용되지 않습니다.

저작권법에 따른 이용자의 권리는 위의 내용에 의하여 영향을 받지 않습니다.

이것은 이용허락규약(Legal Code)을 이해하기 쉽게 요약한 것입니다.

Disclaimer

dCollection

연세대학교
YONSEI UNIVERSITY

Renoprotective effect of haptoglobin and hemopexin by inhibiting ferroptosis in ischemic-reperfusion acute kidney injury

Ye Eun Ko

Department of Medicine

The Graduate School, Yonsei University

연세대학교
YONSEI UNIVERSITY

Renoprotective effect of haptoglobin and hemopexin by inhibiting ferroptosis in ischemic-reperfusion acute kidney injury

Directed by Professor Tae-Hyun Yoo

The Doctoral Dissertation
submitted to the Department of Medicine,
the Graduate School of Yonsei University
in partial fulfillment of the requirements for the degree of
Doctor of Philosophy in Medical Science

Ye Eun Ko

December 2023

연세대학교
YONSEI UNIVERSITY

This certifies that the Doctoral Dissertation of
Ye Eun Ko is approved.

Thesis Supervisor : Tae-Hyun Yoo

Thesis Committee Member#1 : Seung Hyeok Han

Thesis Committee Member#2 : Dong Ki Kim

Thesis Committee Member#3 : Jung Tak Park

Thesis Committee Member#4 : Beom Jin Lim

The Graduate School
Yonsei University

December 2023

연세대학교
YONSEI UNIVERSITY

ACKNOWLEDGEMENTS

I would like to express my deepest gratitude to everyone who contributed to the completion of this thesis.

I extend my heartfelt appreciation to Professor Tae-Hyun Yoo for his meticulous and compassionate guidance, leading me through the entire process. His encouragement played a crucial role in achieving various research tasks. I will forever cherish your words of enthusiasm and kindness in my heart.

I am also very grateful to Professor Shin-Wook Kang and Doctor Hyeok Woo Lee for serving as role models and for their multifaceted supports. Your supports have been indispensable in enabling me to complete this work.

Additionally, I extend my appreciation to Professor Seung Hyeok Han and Professor Jeong Tak Park for his invaluable advice. I would like to acknowledge Professor Dong Ki Kim and Professor Beom Jin Lim for their valuable insights into my research.

I would also like to express my gratitude to Professor Dong-Ryeol Ryu and Professor Hyung Jung Oh for inviting me into the field of research in the first place. I would also like to express my gratitude to Young Su Joo for providing timely guidance.

I extend my heartfelt appreciation to Bo Young Nam for instructing and supporting me throughout the entire experiment and analysis process. Additionally, I express my gratitude to the lab members—Gyuri Kim, Jae Jin Ryu, and Joo Yeon Park—for their patience and support during my graduate school studies. I would like to express my gratitude to Ms. Hyojung Um for her invaluable administrative support and encouragement throughout my research.

I express profound gratitude to my husband, whose unwavering joy and support played a pivotal role in bringing this work to completion. I extend my appreciation to my parents for their hard work and sacrifices, as well as to my brother. Furthermore, I would like to thank my parents-in-law for their unconditional support.

연세대학교
YONSEI UNIVERSITY

<TABLE OF CONTENTS>

연세대학교
YONSEI UNIVERSITY

연세대학교
YONSEI UNIVERSITY

LIST OF FIGURES

연세대학교
YONSEI UNIVERSITY

LIST OF TABLES

연세대학교
YONSEI UNIVERSITY

ABSTRACT

Renoprotective effect of haptoglobin and hemopexin by inhibiting ferroptosis in ischemic-reperfusion acute kidney injury

Ye Eun Ko

Department of Medicine
The Graduate School, Yonsei University

(Directed by Professor Tae-Hyun Yoo)

Background: Recent studies showed that cell free hemoglobin (CFH) increases in patients with sepsis and after heart surgery, which may cause acute kidney injury (AKI). Since CFH contains catalytically active iron, CFH-related ferroptosis, an iron-dependent form of cell death, may induce AKI. This study investigates the renoprotective effects of haptoglobin (Hp) and hemopexin (Hx), which scavenge CFH, in an experimental AKI model in relation to ferroptosis.

Methods: Ischemic-reperfusion injury (IRI) animal models were used as AKI animal models. After 2, 4, 6, 8, and 24 hours, CFH and hemin levels were evaluated in both the control and IRI groups. In addition, the IRI models were treated with different doses (100, 200 mg/kg) of Hp or Hx via intravenous injection 30 minutes after IRI surgery. CFH, hemin, kidney injury markers, and oxidative stress markers, as well as ferroptosis markers were evaluated 24 hours later. Furthermore, kidney injury score was evaluated from kidney tissues based on the percentage of cell necrosis, loss of brush border, cast formation, and tubule dilatation. Quantitative polymerase chain reaction, Western blot analysis, and immunohistochemistry were conducted to assess the mechanism related to ferroptosis.

Results: CFH and hemin levels increased in the IRI group at each hour compared to the control. Injection of Hp decreased CFH levels regardless of the dosage, while injection of Hx decreased hemin levels compared to the IRI group. Creatinine, blood urea nitrogen (BUN), neutrophil gelatinase-associated lipocalin (NGAL), malondialdehyde (MDA)

연세대학교
YONSEI UNIVERSITY

levels, and kidney injury score showed increases in the IRI group compared to the control. Treatment with Hp or Hx resulted in decreases in creatinine, BUN, NGAL, MDA, and kidney injury score across all dosages compared to the IRI group. In the IRI group, the mRNA expression of cystine/glutamate antiporter system Xc^- (*Slc7a11*) decreased compared to the control, while ferritin heavy chain 1 (*Fth1*) increased. However, treatment with Hp or Hx resulted in an increase in *Slc7a11* mRNA expression and a decrease in *Fth1* compared to the IRI group. Additionally, protein expression and the intensity of immunohistochemistry staining for SLC7A11 and GPX4 exhibited a decrease in the IRI group, which was subsequently ameliorated following the administration of Hp or Hx. In contrast, FTH1 displayed the opposite trend.

Conclusions: Hp and Hx may aid as preventive agents for ischemic-reperfusion AKI by inhibiting ferroptosis.

Key words: acute kidney injury, ischemic-reperfusion injury, haptoglobin, hemopexin, kidney protection

연세대학교
YONSEI UNIVERSITY

Renoprotective effect of haptoglobin and hemopexin by inhibiting ferroptosis in ischemic-reperfusion acute kidney injury

Ye Eun Ko

Department of Medicine
The Graduate School, Yonsei University

(Directed by Professor Tae-Hyun Yoo)

I. INTRODUCTION

Acute kidney injury (AKI) is highly prevalent, with an increasing incidence rate, and AKI-associated morbidity and mortality have emerged as serious problems worldwide. [1,2] Even though it is a clinically crucial and serious disease, there are no effective preventive drugs or treatment strategy for AKI. Therefore, research on the mechanisms and mediators of AKI has been continued to develop the therapeutics. Recent studies show that cell free hemoglobin (CFH) increases in sepsis and after heart surgery, [3-6] which may cause AKI. [7] In addition, a study reported that cell free hemoglobin is a prognostic factor for kidney survival in patients with ECMO therapy. [8] These findings suggested that CFH may be causally related with kidney injury.

Recently, ferroptosis, which is a different form of apoptosis and iron-dependent, has been introduced. [9] Several studies showed that ferroptosis is related to the tubular cell death in various types of AKI. [10,11] The cystine/glutamate antiporter system Xc^- (SLC7A11, xCT) and an antioxidant enzyme, glutathione peroxidase 4 (GPX4), play key roles as mediators in ferroptosis. Low xCT and GPX4 levels decrease intracellular cysteine levels, which

연세대학교
YONSEI UNIVERSITY

eventually lower glutathione synthesis and lipid peroxide degradation. These changes cause intracellular lipid peroxide accumulation, and result in ferroptosis. [10,12,13] In AKI animal models, Ferrostatin-1 (Fer-1), which inhibits lipid oxidation and thereafter inhibits ferroptosis, reduced tubular injury. [14,15] Furthermore, studies showed that in GPX4-null mice, interstitial edema, tubular cell death, and proteinuria were significantly increased. [16]

The ischemic-reperfusion injury (IRI) model is one of the frequently used AKI models. AKI that occurs during kidney transplantation and intrarenal IRI that occurs during cardiovascular surgery are very similar models. [17] In IRI, cellular hypoxia and reoxygenation are two significant factors. [18] The imbalance between reactive oxygen species (ROS) production and the competence of cells to detoxify these ROS generates oxidative stress, causing the production of cell damage mediators and resulting in IRI. [19-21] Oxidative stress is known to be an essential element in cellular damage in hypoxia-reoxygenation injury and consequent IRI. [22,23] Oxidative stress causes endothelial damage and, consequently, hemolysis, and elevation of CFH. [24] Since CFH contains catalytically active iron ($Hb\text{-}Fe^{3+}$), which is related to iron-dependent cell death, CFH-related ferroptosis may be induced. [24,25] $Hb\text{-}Fe^{3+}$ releases hemin which results in oxidation of membrane lipids and low-density lipoprotein (LDL), [26] eventually causing ferroptosis. LDL oxidation leads to inflammatory and cytotoxic actions which may induce further vascular injury. [27,28]

Therefore, physiologically, to attenuate this toxicity, extracellular hemoglobin and hemin are removed from the plasma by natural scavenger proteins, haptoglobin (Hp) and hemopexin (Hx). [25,29,30] Hp radically changes the physiologic and biochemical characteristics of CFH by intravascular sequestration, limiting extravascular translocation of CFH, and controlling radical reaction. [31] Recent in vitro studies show that Hp reduces the redox capability of bound $Hb\text{-}Fe^{3+}$ and prevents radical transfer. [32,33] Hx is the most

연세대학교
YONSEI UNIVERSITY

potent hemin-binding protein. Hx limits hemin interaction with cell-surface receptors and protect susceptible lipoproteins from oxidation. [34-36] In hemin treated Hx-knockout mice, scavenger protein showed reduction of hemin-induced endothelial cell activation and kidney injury. [37,38] This suggests the possibility of scavenger protein as a preventive or therapeutic agent for AKI.

The aim of this study is to figure out the renoprotective effect of Hp and Hx, which are scavenger proteins of CFH, and explain its mechanism in relation to ferroptosis in experimental AKI model.

II. MATERIALS AND METHODS

1. Animal study, ischemic-reperfusion injury model and treatment

All animal protocols were approved by the Committee for the Care and Use of Laboratory Animals at Yonsei University College of Medicine in Seoul, Korea. All experiments were conducted as the Guide for the Care and Use of Laboratory Animals, 8th edition (NIH, 2011). C57BL/6J mice (7 weeks old) from The Jackson Laboratory (Bar Harbor, ME, USA) were used in this study. With the body temperature maintained at around 37°C, animals were anesthetized with the mixture of 30 mg/kg of zolazepam (Zoletil 100, Virbac, Carros, France) and 10 mg/kg of xylazine (Rompun 10 mL, Elanco, Ansan-si, Gyeonggi-do, Republic of Korea), in a prone position, and shaved, exposing the kidneys by incision with a flank approach. Renal pedicles were clamped with microvascular clips and then the clips were removed after the ischemia induction time for reperfusion. To determine the optimal timing of Hp or Hx injection, Hp or Hx was injected via tail vein 30 minutes before, 30 minutes after, or both 30 minutes before and after IRI operation at a fixed dose of 100

연세대학교
YONSEI UNIVERSITY

mg/kg. To figure out the optimal dose of Hp or Hx, 30 minutes after IRI operation, Hp or Hx was administered at a dose of 100 mg/kg or 200 mg/kg according to each assigned group. Kidney function, ferroptosis marker and oxidative stress marker were measured 24 hours after IRI surgery.

2. Assessment of kidney function and kidney injury

After anesthetizing the animals by mixture of 30 mg/kg of zolazepam and 10 mg/kg of xylazine, 500-700 μL of blood was collected from the heart tip after central line incision. Blood was injected into EDTA tube, lightly inverted 3 to 4 times, and then put in ice. After centrifuged at 15,000 rpm for 10 minutes at 4°C, upper layer was isolated and referred to other institution for analysis. Plasma creatinine and blood urea nitrogen (Roche, Mannheim, Baden Württemberg, Germany) were analyzed to evaluate kidney function. Kidney tubular injury was assessed by mRNA quantification of the renal epithelial injury biomarker, NGAL (R&D Systems, Minneapolis, MN, USA). The qualitative scoring system of scale from 0 to 4 based on percentage of area with kidney injury was used to evaluate the slides[39,40]; 0= no kidney injury, 1= minimal injury with ≤10% affected, 2= moderate injury with 11-25% affected, 3= significant injury with 26-45% affected, and 4= significant injury with 46-75% affected severe injury with 76-100% affected. More than ten 200x fields per kidney were evaluated.

3. Measurement of cell free hemoglobin, hemin, and lipid peroxidation

Plasma CFH (Sigma–Aldrich, St. Louis, MO, USA) and hemin (Abcam plc, Bristol, UK) were measured 2, 4, 6, 8, 24 hours after IRI. Oxidative stress was measured by lipid peroxidation, malondialdehyde (MDA) levels, using an MDA assay kit (Abcam,

연세대학교
YONSEI UNIVERSITY

Cambridge, MA, USA) for kidney tissue. Whole mouse kidneys were harvested and lysed in lysis solution (MDA lysis buffer and 5% butylated hydroxytoluene), and afterwards, centrifuged at 13,000×g for 10 minutes at 4°C. Supernatants were cleared, and MDA levels were determined using the reaction of thiobarbituric acid at a wavelength of 532nm. The MDA content of each specimen was calculated compared to the standard.

4. Preparation of human hemopexin

Hx was purified using the optimized method as described in patent PCT/KR2022/001519. Human Hx was isolated from human serum Cohn fraction IV paste. Paste was dissoluted in 20 mM sodium citrate pH 7.0 followed by filter-press using 40+30 μm cellulose filter (Ahlstrom, Helsinki, Finland) to remove residual solid particles. Filtrate was purified through Q sepharose (Cytiva, Marlborough, MA, USA) and Toyopearl DEAE (TOSOH, Tokyo, Japan) then subsequently immobilized in Nickel sepharose resin (Cytiva, Marlborough, MA, USA). The column was rinsed with 20 mM sodium phosphate, 500 mM sodium chloride, pH 7.4 containing 20 mM imidazole to remove any non-specifically bound impurities. Hx was eluted with same buffer except that 60 mM imidazole was contained. Hx was further purified by passing through the Phenyl sepharose (Cytiva, Marlborough, MA, USA) column in 10 mM sodium phosphate, 1.2 M sodium chloride pH 7.0. The final purified Hx was concentrated and formulated in 10 mM sodium phosphate, 150 mM sodium chloride pH 7.0. The purity of human Hx (>95%) was analyzed by sodium dodecyl-sulfate polyacrylamide gel electrophoresis (SDS-PAGE) and size exclusion chromatography (SEC).

연세대학교
YONSEI UNIVERSITY

5. Preparation of human haptoglobin

Hp was purified using the optimized method as described in patent PCT/KR2022/001519. Human Hp was isolated from human serum Cohn fraction IV paste equal to that of Hx isolation. Hp purification shared same process to the Hx from dissolution to Q sepharose (Cytiva, Marlborough, MA, USA). Hp was immobilized in Toyopearl DEAE resin (TOSOH, Tokyo, Japan), rinsed with 5 mM sodium citrate, pH 5.9, eluted with 5 mM sodium citrate, 50 mM sodium chloride, pH 5.9. Phenyl resin (Cytiva, Marlborough, MA, USA) was used in the bind-elution mode within ammonium sulfate salt for further purification. The final purified Hp was concentrated and formulated in 10 mM sodium phosphate, 150 mM sodium chloride pH 7.0. The purified human Hp was analyzed by SDS-PAGE and specific activity.

6. SDS polyacrylamide gel electrophoresis (SDS-PAGE)

Hp sample of non-reduction conditions was analyzed using NuPage 3-8% Tris-acetate gel (Thermo Fisher Scientific Inc., Waltham, MA, USA). The reduction conditions of the Hp sample and the non-reduction/reduction conditions of the Hx sample were analyzed using the NuPage 4-12% bis-tris gel (Thermo Fisher Scientific Inc., Waltham, MA, USA).

7. Size exclusion chromatography (SEC)

Molecular integrities of purified human Hx and Hp were assessed with TSKgel G3000SWxl column (TOSOH, Tokyo, Japan) connected with Waters e2695 Separation module (Waters, Milford, MA, USA). Absorption data was collected by using Waters 2489 UV/Vis Detector (Waters, Milford, MA, USA) controlled by Empower software. Mobile phase used for molecular integrity evaluation was phosphate-buffered saline (PBS). The

연세대학교
YONSEI UNIVERSITY

injection volume of each protein sample was 50 μL and the detection was performed in 280 nm.

8. Specific activity of haptoglobin

Specific activity of Hp was assessed by calculating the amount of Hp content in total protein, expressed in percentage. Measurements of Hp and total protein were done by ELISA and Bradford assay.

9. Haptoglobin quantification by Sandwich-ELISA

Quantification of human Hp was performed by using Human Hp ELISA Kit (AVIVA, San Diego, CA, USA). Standards and samples were added to plates pre-coated with specific antibodies to human Hp and incubated for 15 min at 37℃ in dark. Unbound and free molecules were washed away using the wash buffer supplied with the kit. Enzyme-antibody conjugate specific for human Hp was added to the plate and was incubated for 15 min at 37℃ in dark. The substrate solution was added to each well after unbound molecules were washed away. Enzyme substrate reaction was blocked by adding blocking solution subsequently to 5 min incubation at 37℃ in dark. The absorbance at 450 nm for each well was measured by spectrophotometer. Standard curve was constructed and concentration of human Hp was calculated by converting absorbance data collected to ng/mL.

10. Bradford assay

The quantitation of protein was carried out by Bradford assay. The assay was performed by adding predetermined amounts of Bradford assay reagent (Thermo Fisher Scientific Inc., Waltham, MA, USA) to the samples and standards added on to 96-well plate. The

연세대학교
YONSEI UNIVERSITY

absorbance at 595 nm for each well was measured using a spectrophotometer. The calibration curve of the concentration between 62.5-1000 μg/mL was constructed and the concentration of the sample was calculated by converting the absorbance data collected to μg/mL.

11. Total RNA extraction

The pieces of mouse kidney samples were rapidly frozen using liquid nitrogen and then homogenized with 700 μL RNAiso reagent using a mortar and pestle, performing three rounds of homogenization. Following homogenization, 160 μL of chloroform was added to the kidney samples. The mixtures were incubated at 4°C for 15 minutes. After the incubation, the samples were centrifuged at 15,000 rpm for 15 minutes at 4°C. This step resulted in the separation of three layers, and the top layer (aqueous layer) was carefully transferred to a fresh tube. To precipitate the RNA, 400 μL of isopropanol was added to the transferred aqueous layer. The tube was then centrifuged at 15,000 rpm for 15 minutes at 4°C after overnight incubation at -20°C. The RNA pellet obtained after centrifugation was washed with 1 mL of 70% ethanol and allowed to air-dry. Finally, the RNA pellet was dissolved in sterile diethyl pyrocarbonate-treated distilled water. The quantity and quality of the extracted RNA were evaluated using spectrophotometric measurements at wavelengths of 260 nm.

12. Reverse transcription

The first-strand complementary DNA (cDNA) was generated from the extracted RNA using the cDNA synthesis kit (Takara Bio). For this process, two micrograms of total RNA were reverse transcribed. The reverse transcription reaction included a 10 μM random

연세대학교
YONSEI UNIVERSITY

hexanucleotide primer, 1 mM dNTP, 8 mM MgCl2, 30 mM KCl, 50 mM Tris-HCl at pH 8.5, 0.2 mM dithiothreitol, 25 U RNase inhibitor, and 40 U PrimeScript reverse transcriptase. The mixture was then incubated at 30°C for 10 minutes, followed by 1 hour of incubation at 42°C. Finally, the enzyme was inactivated by incubating the mixture for 5 minutes at 99°C.

13. Real time quantitative polymerase chain reaction

The quantitative real-time polymerase chain reaction (qPCR) was carried out in a 20 μL reaction mixture. This mixture included 10 μL of SYBR Green PCR Master Mix (Applied Biosystems, Foster City, CA, USA), 5 μL of reverse transcribed cDNA, and 5 pM concentrations of both sense and antisense primers. The primer sequences are listed in Table 1. These primer concentrations were optimized through preliminary experiments to ensure their ideal amounts. The qPCR process started with an initial heating step of 9 minutes at 95°C, followed by repetitive cycles. Each cycle consisted of denaturation for 30 seconds at 94.5°C, annealing for 30 seconds at 60°C, and extension for 1 minute at 72°C. A final extension was performed for 7 minutes at 72°C. To ensure accuracy, each sample was run in triplicate using separate tubes. Following qPCR, a melting curve was constructed by gradually increasing the temperature from 60 to 95°C at a rate of 2°C per minute. The cDNA content of each sample was determined using a comparative CT method with $2^{-\Delta\Delta CT}$. The results were expressed as relative expression levels normalized to the expression of 18s ribosomal RNA (rRNA) and presented in arbitrary units. The qPCR analysis aimed to compare the transcript levels of genes related to ferroptosis (*Slc7a11*, *Gpx4*, *Fth1*). All primers used in the study were obtained from Applied Biosystems.

연세대학교
YONSEI UNIVERSITY

Table 1. Primer sequences

Mouse Gene	Sequence (5'→ 3')	
Slc7a11	Forward	TGA ATG CCT TGT CTG CTT TG
	Reverse	GAA TTG CAG GGA ACT GTG GT
Gpx4	Forward	AGA TCC ACG AAT GTC CCA AG
	Reverse	CCT CCT CCT TAA ACG CAC AC
Fth1	Forward	TGA TGT GGC CCT GAA GAA C
	Reverse	TCA TCA CGG TCA GGT TTC TG
18s	Forward	CGC TTC CTT ACC TGG TTG AT
	Reverse	GGC CGT GCG TAC TTA GAC AT

14. Western blot analysis

Western blot analysis was conducted following the previously described method.[41] For this analysis, primary antibodies were employed, including polyclonal antibodies against SLC7A11 (ab37185, Abcam), GPX4 (ab125066, Abcam), ferritin heavy chain 1 (FTH1, #3998, Cell Signaling Technology), and β-actin (A5441, Sigma-Aldrich). Subsequently, the membranes were subjected to three washes for 10 minutes each in Tris-buffered saline with 0.1% Tween-20 and then placed in buffer A, which contained a 1:1000 dilution of horseradish peroxidase-conjugated goat-anti-rabbit or anti-mouse IgG (GenDEPOT, Barker, TX, USA). To quantify the band intensities, ImageJ software (NIH, Bethesda, MD, USA) was used, and changes in the treated groups were compared to control tissues for further analysis.

15. Histological analysis

Histological evaluation of kidney sections fixed in 10% formalin and embedded in

연세대학교
YONSEI UNIVERSITY

paraffin was conducted using Periodic acid-Schiff (PAS) and Masson's trichrome staining.

For PAS staining, the tissue slides were treated with dissolved paraffin in an incubator at 60°C for over an hour. Subsequently, the slides were rehydrated in a sequential manner using xylene, 100%, 95%, and 90% alcohol. After washing the slides with distilled water, they were immersed in periodic acid for 7 minutes, followed by a 15-minute reaction in Schiff's solution. Modified Mayer's Hematoxylin counter-staining was then performed after dehydration.

Regarding Masson's trichrome (MT) staining, 5 μm-thick sections of paraffin-embedded tissues were deparaffinized and rehydrated using ethyl alcohol. The samples were then washed in tap water and re-fixed in Bouin's solution for an hour at 56°C. After washing the samples with running tap water for 10 minutes, they were stained with Weigert iron hematoxylin working solution for 10 minutes. Next, the slides were treated with Biebrich scarlet-acid fuchsin solution for 15 minutes and washed in tap water. The sections were differentiated in phosphomolybdic-phosphotungstic acid solution for 15 minutes, transferred to aniline blue solution, and stained for 10 minutes. Following a brief rinse in tap water, the sections were reacted with a 1% acetic acid solution for 5 minutes. Quantitative analysis of the stained images was performed to assess the percentage of positive staining in the areas corresponding to PAS (purple) and MT (sky-blue and blue colors). This analysis was carried out using the color-deconvolution plugin and area fraction/area measurements through the Image J software.

16. Immunohistochemistry

Kidney samples were immersed in a solution of 10% neutral-buffered formalin to achieve fixation. Subsequently, the specimens were processed into sections measuring 5

연세대학교
YONSEI UNIVERSITY

μm in thickness, a preparation required for the subsequent immunohistochemical analysis. The tissue sections underwent a series of steps including deparaffinization, rehydration in ethyl alcohol, and a final rinse in tap water. To facilitate antigen retrieval, a solution of 10 mM sodium citrate buffer was employed for a duration of 20 minutes within a Black & Decker vegetable steamer. To prevent nonspecific binding, the prepared slides were treated with a blocking solution containing 10% donkey serum for a span of 1 hour at room temperature (RT). Following this, a thorough wash using PBS was conducted. Primary antibodies directed against SLC7A11 (ab37185, Abcam), GPX4 (ab125066, Abcam), FTH1 (Cell Signaling Technology), MDA (ab6463, Abcam), and 4-hydroxynonenal (4-HNE; ab46545, Abcam) were appropriately diluted in a mixture of 2% casein and bovine serum albumin. These antibody solutions were subsequently applied to the slides, which were then subjected to an overnight incubation at a temperature of 4°C. After the incubation, washing was performed, and a secondary antibody (Dako, Carpinteria, CA, USA) was applied for a duration of 1 hour at RT. Detection was achieved by introducing diaminobenzidine for a duration of 2 minutes, followed by counterstaining with hematoxylin. For assessing staining intensity, at least five fields within each section under a magnification of 200x were examined.

17. Iron assay

The levels of total iron within tissues were evaluated by employing an iron assay kit (Sigma-Aldrich). For this assessment, mouse kidney tissue samples (30 mg) were collected and then homogenized in an iron assay buffer. Following homogenization, all samples underwent centrifugation at 16,000×g for 10 minutes. Then, 30 μL of supernatant was combined with 70 μL of the iron assay buffer for each sample. Subsequently, 5 μL of an

연세대학교
YONSEI UNIVERSITY

iron reducer was introduced to each supernatant. The mixture was incubated for a duration of 30 minutes, and the total iron levels were determined by employing an iron probe at a wavelength of 593 nm.

18. Glutathione assay

The glutathione concentration was assessed using a Glutathione Assay Kit (Invitrogen). Mouse kidney samples (10 mg) were harvested, lysed in 250 μL of 100 mM phosphate buffer (pH 7.0), and centrifuged at 14,000 rpm for 10 minutes. The resulting supernatant was collected for protein quantification. Subsequently, an equal volume of supernatant of 5% 5-sulfosalicylic acid (5-SSA) solution was added, followed by centrifugation under the same conditions. The supernatant from each sample was then mixed with 1.5 times the volume of assay buffer. The detection mixture and reaction mixture, including NADPH solution, were introduced into each well and incubated at RT for 20 minutes. Glutathione levels were determined by measuring absorbance at a wavelength of 405 nm. The glutathione content for each sample was determined by comparing it to a standard reference.

19. Statistical analysis

Statistical analysis was conducted using GraphPad Prism 10.3 (GraphPad, San Diego, CA, USA). For comparison between two groups, a student's t-test was performed. A one-factor analysis for variance (ANOVA) was used for comparison among more than 3 groups and followed by the post-hoc Turkey test. P value less than 0.05 was considered statistically significant.

연세대학교
YONSEI UNIVERSITY

III. RESULTS

1. Cell free hemoglobin and hemin elevation after IRI operation and subsequent alteration in kidney function

To assess the impact of IRI in the animal model, CFH and hemin levels were evaluated at various time points (2, 4, 6, 8, and 24 hours) following the IRI procedure. In comparison to the control group that underwent sham operation, the IRI operation model exhibited a statistically significant increase in CFH and hemin levels (Figure 1A).

Furthermore, to assess the influence of IRI on kidney function and oxidative stress markers in the animal model, we measured BUN and creatinine levels at 4, 8, and 24 hours after the IRI procedure. The results revealed elevated levels of BUN and creatinine, indicating a deterioration in kidney function in IRI group, in contrast to the sham operation control group (Figure 1B).

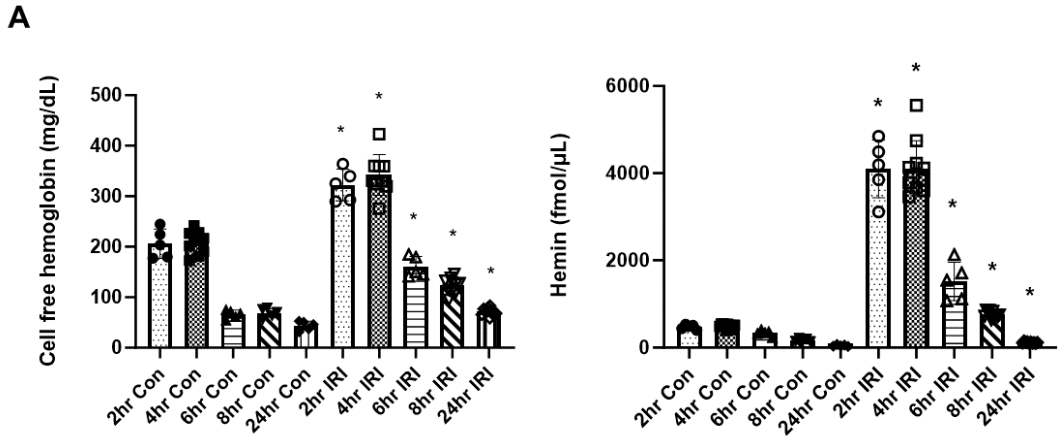

연세대학교
YONSEI UNIVERSITY

B

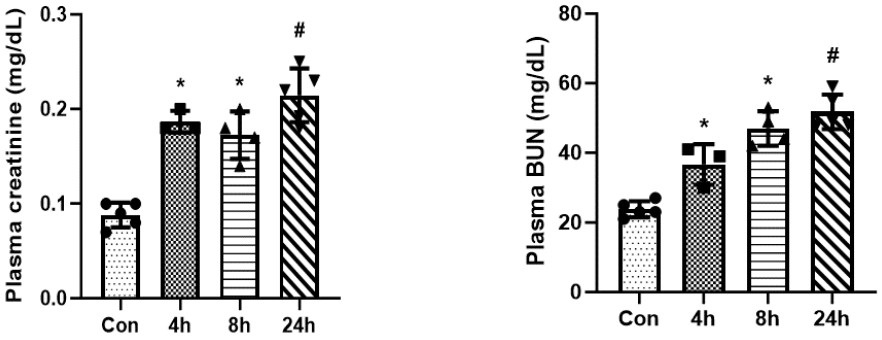

Figure 1. Cell free hemoglobin and hemin elevation after IRI operation and subsequent alteration in kidney function. 2, 4, 6, 8, 24 hours after IRI operation, CFH and hemin level were evaluated. Compared to sham operation control group, IRI operation model showed statistically significant increase in CFH and hemin (A). 4, 8, 24 hours after IRI operation, there was increase in BUN, and creatinine indicating a deterioration in kidney function when compared to the sham operation control group (B). For all groups, data are means ± SD. (*, P <0.0001 vs *sham control*; #, P <0.001 vs. *sham contro*l.)

2. Optimal timing of administration of haptoglobin and hemopexin: before, after, or both before and after IRI operation

To determine the optimal timing of Hp or Hx injection, Hp or Hx was administered at a fixed dose of 100 mg/kg, before, after, or both before and after IRI surgery. Compared to the control group, plasma creatinine, BUN, and NGAL increased in the group that underwent IRI surgery. Compared to the group that underwent IRI surgery, plasma creatinine, BUN, and NGAL decreased statistically significantly in all groups administered Hp or Hx before, after, and both before and after IRI surgery. Overall, the administration of Hp or Hx demonstrated a significant effect, irrespective of the timing of injection. Therefore, I decided to administer the drugs after IRI surgery, taking into consideration the convenience of the experiment.

연세대학교
YONSEI UNIVERSITY

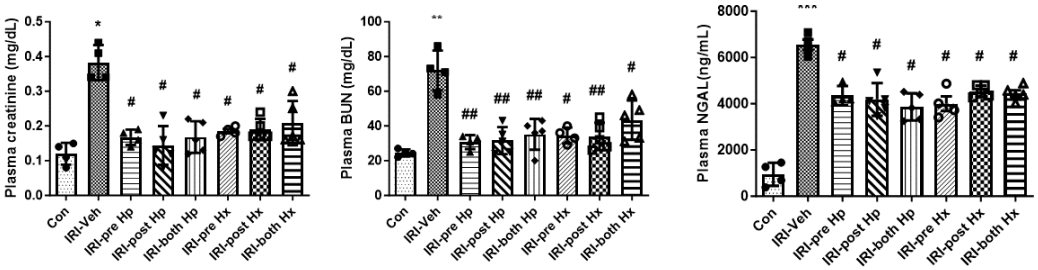

Figure 2. Optimal timing of administration of Hp and Hx: before, after, or both before and after IRI operation. Through the administration of Hp and Hx before, after, or both before and after the IRI, enhancements in kidney function were observed within the IRI model, with no statistically significant differences noted among the various timing approaches. For all groups, data are means ± SD. (*; P<0.05 vs. *sham control*, **; P<0.01 vs. *sham control*, ***; P<0.001 vs. *sham control*, #; P <0.05 vs. *IRI-vehicle*, ##; P <0.01 vs. *IRI-vehicle*.)

3. The attenuation of elevated cell free hemoglobin and hemin levels in the IRI model after haptoglobin and hemopexin treatment leading to a subsequent improvement in kidney function

To validate the hypothesis that Hp, a scavenger protein for CFH, and Hx, a scavenger protein for hemin, could lead to a reduction in CFH and hemin levels and consequently influence kidney function and oxidative stress, intravenous injections of Hp or Hx were administered to the IRI model via the tail vein 30 minutes after the IRI surgery, using different doses (100 and 200 mg/kg). The injection of Hp resulted in a decrease in CFH levels, independent of the dosage, while the injection of Hx led to reduced hemin levels compared to the IRI group. Furthermore, treatment with either Hp or Hx resulted in lowered creatinine, BUN, and NGAL levels across all dosages compared to the IRI group.

연세대학교
YONSEI UNIVERSITY

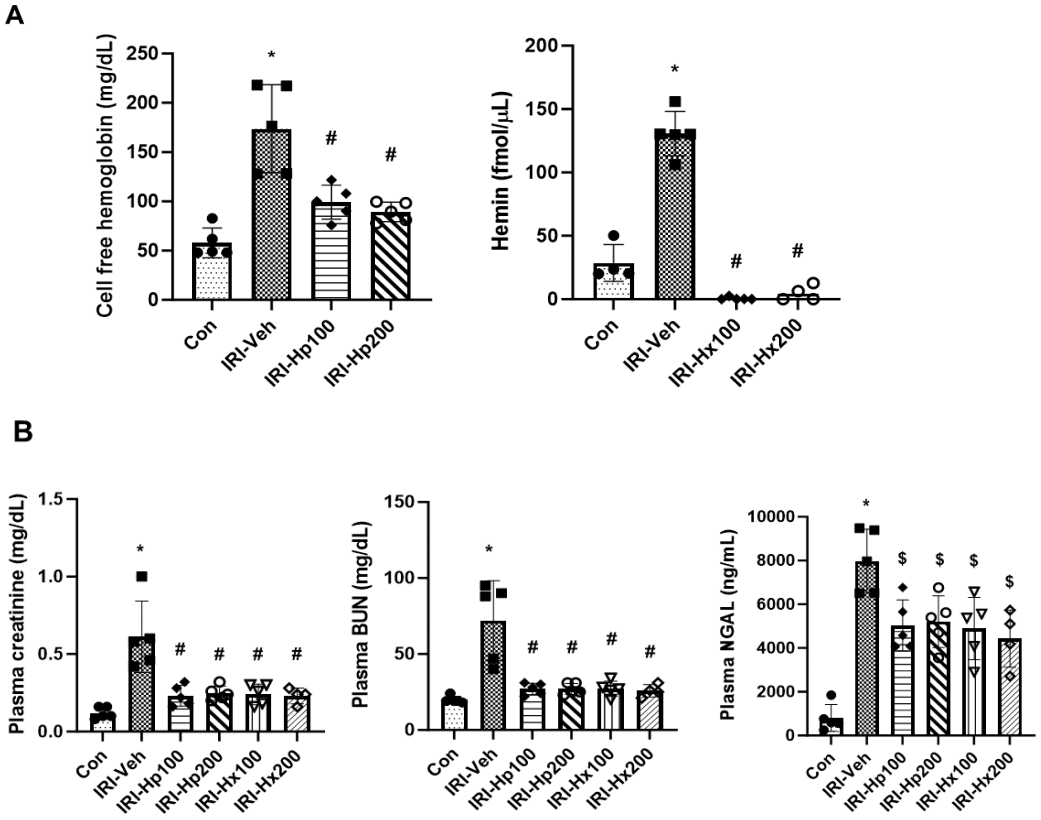

Figure 3. The attenuation of elevated cell free hemoglobin and hemin levels in the IRI model after haptoglobin and hemopexin treatment leading to a subsequent improvement in kidney function. Hp or Hx was intravascularly injected to IRI model with different doses (100, 200 mg/kg) 30 minutes after IRI surgery (A) Injection of Hp decreased CFH levels regardless of the dosage, while injection of Hx decreased hemin levels compared to the IRI group. (B) Treatment with Hp or Hx resulted in decreases in creatinine, BUN, and NGAL levels across all dosage compared to the IRI group. For all groups, data are means ± SD. (*, P<0.001 vs *sham control*; #, P<0.0001 vs. *IRI-vehicle*; $, P<0.001 vs. *IRI-vehicle*.)

4. The amelioration of kidney injury score following haptoglobin and hemopexin treatment

The kidney injury score, which takes into account the percentage of cell necrosis, loss of brush border, cast formation, and tubule dilatation in kidney tissues, exhibited an increase

연세대학교
YONSEI UNIVERSITY

in the IRI operation group compared to the sham control group. However, treatment with Hp or Hx in the IRI model led to a notable improvement in the kidney injury score. A similar tendency occurred using another type of ischemic-reperfusion kidney injury scoring called EGTI scoring (Figure 4). [42]

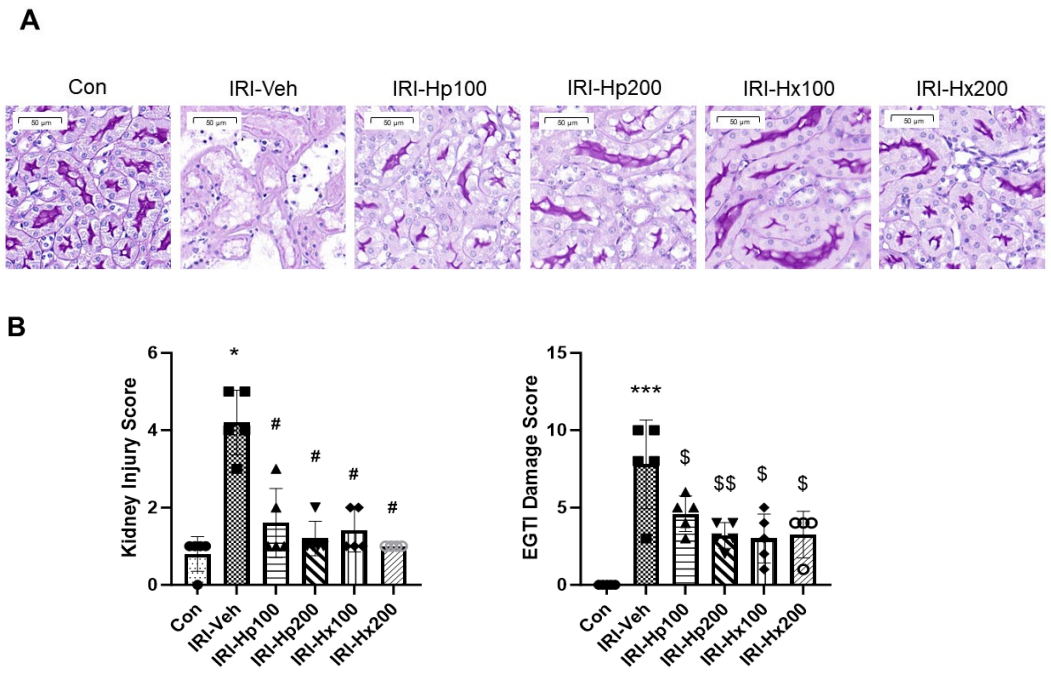

Figure 4. The improvement of kidney injury score after haptoglobin or hemopexin treatment. (A) Kidney tissues were subjected to PAS staining. Representative microscopic images are shown. Scale bar=50 μm. Control, IRI, Hp (100, 200mg/kg) treated IRI model, and Hx (100, 200mg/kg) treated IRI model. (B) Kidney injury score and EGTI damage score were assessed based on histology. Kidney injury score: cell necrosis, loss of brush border, cast formation, tubule dilatation 0: none, 1: ≤ 10% 2: 11-25% 3: 26-45% 4: 46-75% 5: ≥76%. For all groups, data are means ± SD. (*; *P*<0.01 vs. *sham control*, ***; *P*<0.0005 vs. *sham control,* #; *P* <0.005 vs. *IRI-vehicle,* $; *P* <0.05 vs. *IRI-vehicle*, $$; *P* <0.001 vs. *IRI-vehicle.*)

5. Assessment of ferroptosis markers across multiple groups: the control, IRI group, and haptoglobin or hemopexin administration after IRI at varying doses

In order to substantiate the hypothesis that scavenger proteins, Hp or Hx, could attenuate

연세대학교
YONSEI UNIVERSITY

ferroptosis activation caused by CFH and hemin induced by IRI, an evaluation of key ferroptosis markers by qPCR was conducted, including *Slc7a11*, *Gpx4*, and *Fth1*. As per current knowledge, ferroptosis activation is associated with a decrease in *Slc7a11* and *Gpx4* levels, and an increase in *Fth1* expression. Consequently, in the IRI group, the mRNA expression of *Slc7a11* decreased in comparison to the control group, while the expression of *Fth1* increased. However, treatment with Hp or Hx led to an increase in *Slc7a11* mRNA expression and a decrease in *Fth1* expression when compared to the IRI group (Figure 5A). Western blot analysis was done for SLC7A11, GPX4, and FTH1. As in qPCR mRNA expression analysis, protein analysis also showed decrease in SLC7A11 and GPX4 protein expression in IRI group, and an increase in FTH1 expression. Treatment with Hp or Hx ameliorated these changes (Figure 5B, 5C). In addition, immunohistochemistry was conducted to further investigate the underlying mechanism. The immunohistochemical staining for SLC7A11 and GPX4 exhibited reduced intensity in the IRI group, whereas the intensity of FTH1 increased. These alterations were reversed following the administration of Hp or Hx (Figure 5D).

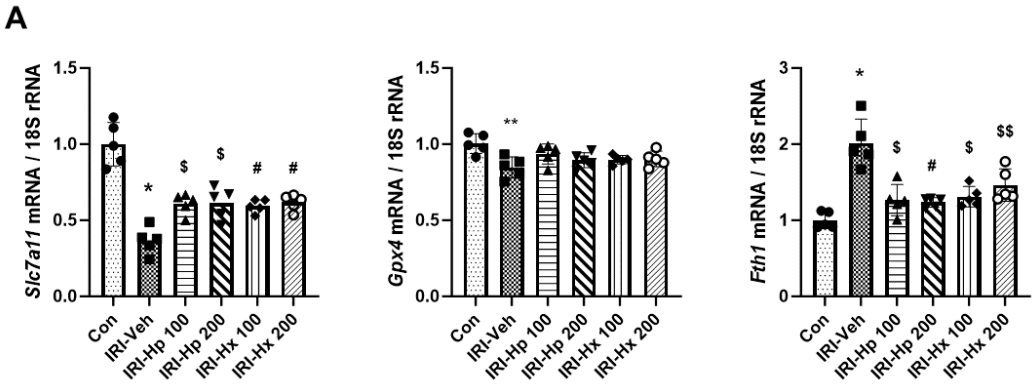

연세대학교
YONSEI UNIVERSITY

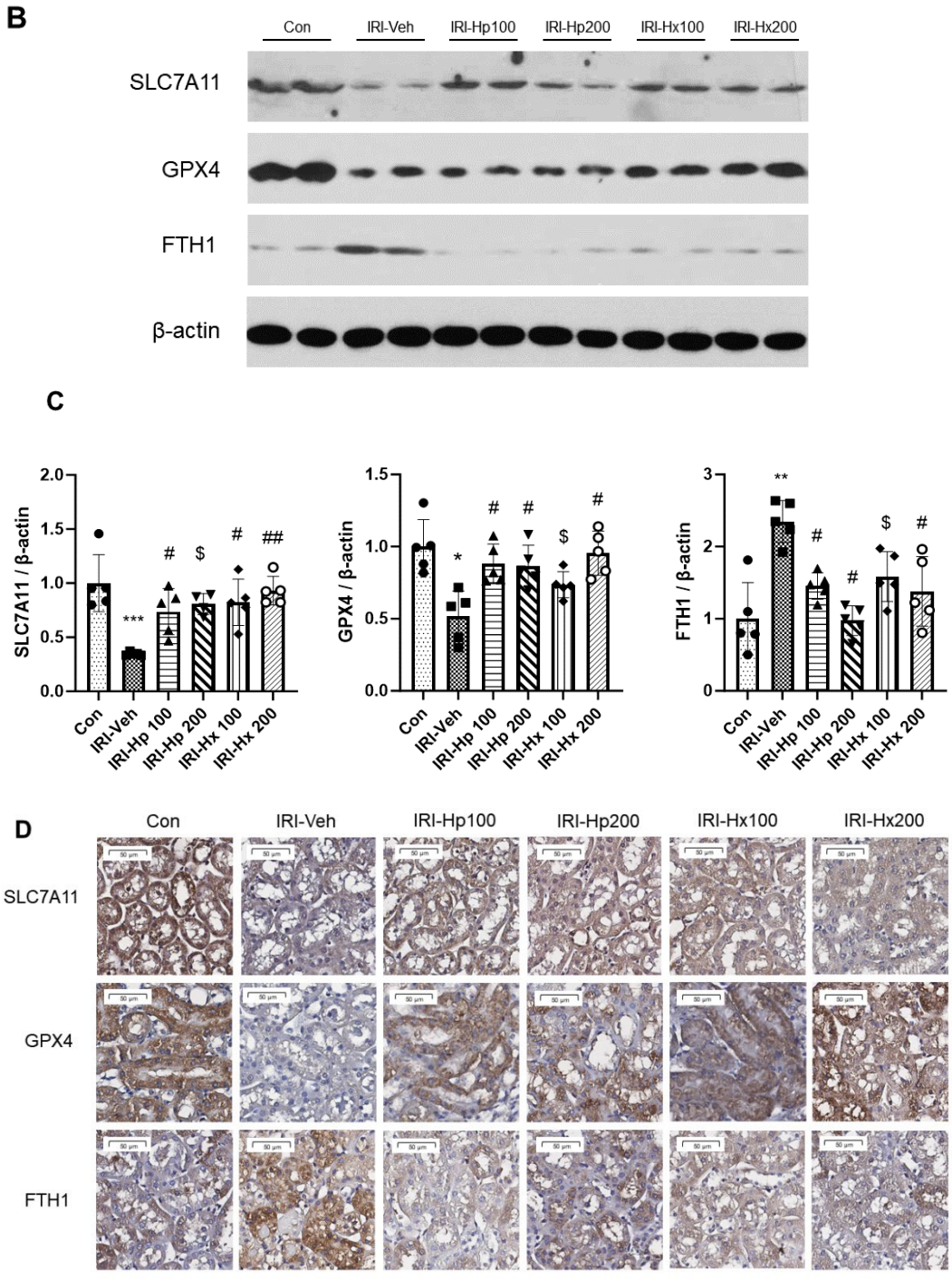

연세대학교
YONSEI UNIVERSITY

Figure 5. The comparison of ferroptosis markers among the control group, the IRI group, and different administration doses (100 mg/kg, 200 mg/kg) of haptoglobin or hemopexin injection after IRI. (A) In the IRI group, the mRNA expression of *Slc7a11* decreased compared to the control, while *Fth1* increased. However, treatment with Hp or Hx resulted in an increase in *Slc7a11* mRNA expression and a decrease in *Fth1* mRNA expression compared to the IRI group. (B, C) Similar to the qPCR mRNA expression analysis, the protein analysis indicated a decrease in the protein expression of SLC7A11 and GPX4 in the IRI group, along with an increase in FTH1 expression. The administration of Hp or Hx resulted in the reversal of these alterations. (D) The immunohistochemical staining of SLC7A11 and GPX4 showed decreased intensity in the IRI group, while the intensity of FTH1 increased. These changes were reversed with the administration of Hp or Hx. For all groups, data are means ± SD. (*, P<0.0001 vs *sham control*; **, P<0.01 vs. *sham control*; ***, P<0.005 vs. *sham control,* $$, P<0.005 vs. *IRI-vehicle*; $, P<0.05 vs. *IRI-vehicle; #*, P<0.001 vs. *IRI-vehicle, ##*, P<0.0001 vs. *IRI-vehicle.*)

6. Evaluation of iron-dependent cell death, ferroptosis, in relation to lipid peroxidation

In addition to evaluating the increase in systemic CFH in the plasma, the iron content—a possible consequence of CFH and a source of ferroptosis—was also measured in the target organ, kidney tissue. Iron levels increased in the IRI group, and this increase was statistically significantly decreased after the injection of Hp or Hx (Figure 6A). Glutathione levels, which decrease during the activation of ferroptosis, were also measured in the kidney tissue. The glutathione levels decreased in the IRI group but increased after Hp or Hx treatment with statistical significance, aligning with the expectations (Figure 6A).

To assess lipid peroxidation, MDA levels were measured in mouse kidney tissue. Following IRI, MDA increased over time, and regardless of the timing, dose, or treatment with Hp or Hx, MDA levels decreased after treatment (Figure 6B). This was further confirmed through immunohistochemistry analysis of MDA and another lipid peroxidation marker, 4-HNE, which demonstrated an increase in intensity after IRI and a subsequent decrease following treatment with Hp or Hx (Figure 6C).

연세대학교
YONSEI UNIVERSITY

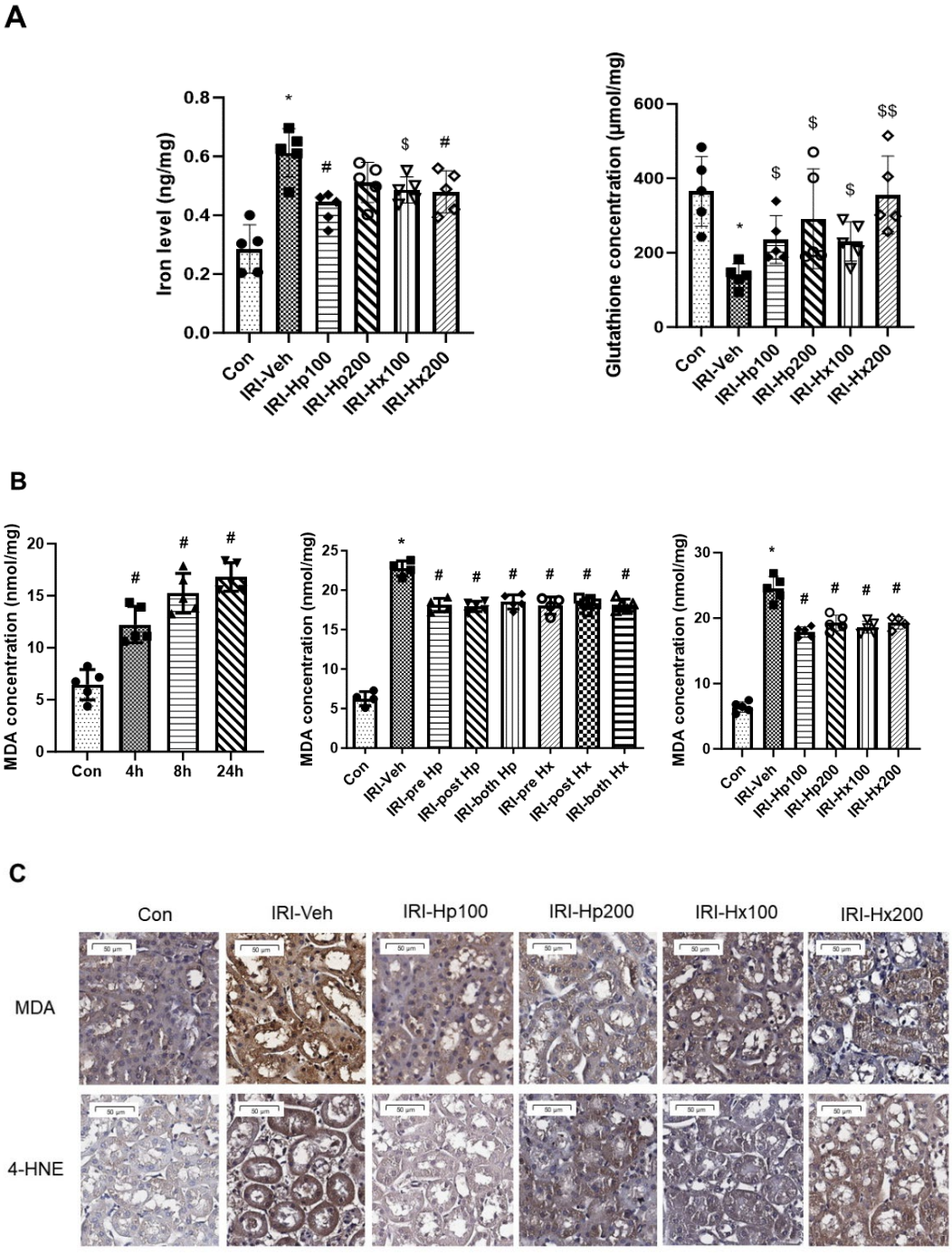

연세대학교
YONSEI UNIVERSITY

Figure 6. Evaluation of iron dependent cell death, ferroptosis, in relation to lipid peroxidation. (A) Iron levels increased in the IRI group, and this increase showed a statistically significant reduction after the administration of Hp or Hx. Conversely, glutathione levels decreased in the IRI group and increased after the administration of Hp or Hx injections. (B) After the induction of IRI, MDA levels exhibited a time-dependent increase. However, irrespective of the timing, dosage, or treatment with Hp or Hx, MDA levels decreased following treatment. (C) Immunohistochemistry analysis of MDA and 4-HNE indicated an intensification in staining after IRI and a subsequent reduction following the administration of Hp or Hx. For all groups, data are means ± SD. (*, $P<0.0001$ vs *sham control*; $$, $P<0.005$ vs. *IRI-vehicle*; $, $P<0.05$ vs. *IRI-vehicle;* #, $P<0.001$ vs. *IRI-vehicle.*)

IV. DISCUSSION

Physiologically, approximately 66% of AKI are induced by IRI or acute tubular necrosis. [43] Causes of IRI include conditions such as myocardial infarction, cardiovascular surgery, and kidney surgery, including kidney transplantation.

In current study, after IRI, elevation of CFH and hemin, deterioration in kidney function and increased oxidative stress marker were observed in animal model. Administration of Hp or Hx was associated with a reduction in CFH or hemin levels, along with an improvement of kidney function, and kidney injury scores. The alteration in the ferroptosis marker, iron, glutathione, and oxidative stress marker level following IRI was attenuated upon the injection of Hp or Hx.

This study may support the idea that IRI can lead to endothelial damage, resulting in hemolysis during the extravasation of red blood cells. This, in turn, leads to the release of cell free hemoglobin, which could potentially cause kidney injury through the mechanism of ferroptosis. However, the effects of this process may be ameliorated through treatment with CFH scavenger proteins such as haptoglobin and heme scavenger proteins like hemopexin (Figure 7).

연세대학교
YONSEI UNIVERSITY

Ischemia leads to the depletion of ATP in cells, which results in the inhibition of the Na^+/K^+ pump, ultimately leading to the intracellular accumulation of Na^+, Ca^{2+}, and cellular edema. This results in the activation of enzymes, such as proteases, and an increase in reactive oxygen species. Additionally, ischemia leads to acidosis, which may cause lysosomal instability and the subsequent release of lysosomal enzymes. All these factors together may lead to cellular membrane injury, resulting in necrosis or apoptosis. Reperfusion, when it occurs, worsens these reactions, causing an increase in reactive oxygen species. The normalization of pH leads to calcium overload, which in turn activates proteases. [44] This is similar to the consequence of a septic condition, involving the activation of inflammatory cytokines and an increase in reactive oxygen species, which can lead to cell injury, including endothelial cells. Endothelial cell damage can lead to hemolysis, resulting in the release of CFH, which may increase free iron levels. In this study, this excess iron is shown to contribute to iron-dependent cell death, specifically ferroptosis. Ferroptosis, in turn, leads to lipid peroxidation, cell injury, and ultimately, kidney damage. The scavenging of iron sources, such as CFH and heme, by haptoglobin and hemopexin, may mitigate the occurrence of ferroptosis.

The limitation of this study is the lack of evaluation of the contribution of the ferroptosis pathway among various types of cell death pathways. Apoptosis is a well-known major cell death signaling pathway, and as previously described, it may be related to the initial increase in CFH. Therefore, excluding the actual impact of apoptosis in the IRI model is not physiologically accurate. However, this condition may be achieved in an in vitro setting by using a pan-apoptosis inhibitor, such as a pan-caspase inhibitor, which was not done in this study.

Nevertheless, the strength of this study lies in establishing a connection between CFH

연세대학교
YONSEI UNIVERSITY

and adverse kidney outcomes. However, there was still a lack of understanding regarding the underlying mechanism. Therefore, this study may serve as a bridge connecting CFH to kidney injury, particularly in the context of ferroptosis. Additionally, it may highlight the potential therapeutic role of haptoglobin and hemopexin in preventing ischemic-reperfusion associated kidney injury.

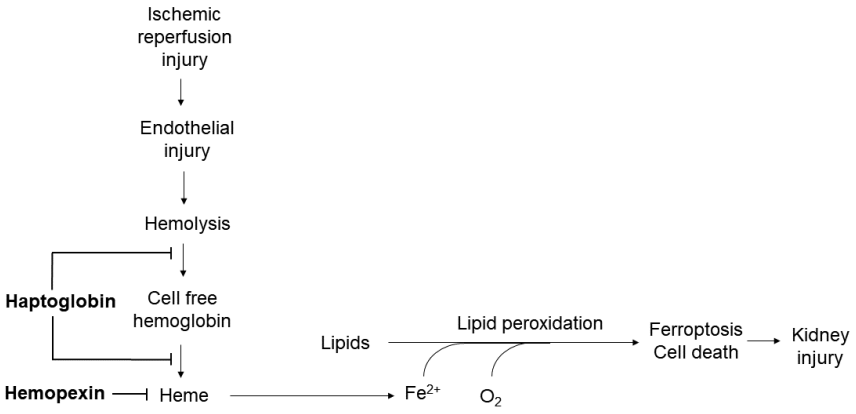

Figure 7. Schematic diagram for hypothesis of renoprotective effect of haptoglobin and hemopexin by inhibiting ferroptosis from IRI model.

V. CONCLUSION

In this study, I demonstrated that Hp and Hx treatment improved the impaired kidney function in IRI operated mice. Treatment with Hp and Hx also resulted in changes to the ferroptosis marker. Thus, scavenger proteins Hp and Hx have the potential to serve as preventive agents against ischemic-reperfusion associated AKI by exerting inhibitory effects on ferroptosis.

연세대학교
YONSEI UNIVERSITY

REFRENCES

1. Sawhney S, Bell S, Black C, Christiansen CF, Heide-Jørgensen U, Jensen SK, et al. Harmonization of epidemiology of acute kidney injury and acute kidney disease produces comparable findings across four geographic populations. Kidney International 2022;101:1271-81.
2. Bolisetty S, Zarjou A, Agarwal A. Heme Oxygenase 1 as a Therapeutic Target in Acute Kidney Injury. American Journal of Kidney Diseases 2017;69:531-45.
3. Larsen R, Gozzelino R, Jeney V, Tokaji L, Bozza FA, Japiassú AM, et al. A Central Role for Free Heme in the Pathogenesis of Severe Sepsis. Science Translational Medicine 2010;2:51ra71-51ra71.
4. Janz DR, Bastarache JA, Peterson JF, Sills G, Wickersham N, May AK, et al. Association between cell-free hemoglobin, acetaminophen, and mortality in patients with sepsis: an observational study. Critical care medicine 2013;41:784.
5. Vermeulen Windsant IC, de Wit NC, Sertorio JT, van Bijnen AA, Ganushchak YM, Heijmans JH, et al. Hemolysis during cardiac surgery is associated with increased intravascular nitric oxide consumption and perioperative kidney and intestinal tissue damage. Frontiers in physiology 2014;5:340.
6. Rezoagli E, Ichinose F, Strelow S, Roy N, Shelton K, Matsumine R, et al. Pulmonary and systemic vascular resistances after cardiopulmonary bypass: role of hemolysis. Journal of Cardiothoracic and Vascular Anesthesia 2017;31:505-15.
7. Windsant ICV, Snoeijs MG, Hanssen SJ, Altintas S, Heijmans JH, Koeppel TA, et al. Hemolysis is associated with acute kidney injury during major aortic surgery. Kidney international 2010;77:913-20.
8. Graw JA, Hildebrandt P, Krannich A, Balzer F, Spies C, Francis RC, et al. The role of cell-free hemoglobin and haptoglobin in acute kidney injury in critically ill adults with ARDS and therapy with VV ECMO. Critical Care 2022;26:50.
9. Dixon SJ, Lemberg KM, Lamprecht MR, Skouta R, Zaitsev EM, Gleason CE, et al. Ferroptosis: an iron-dependent form of nonapoptotic cell death. cell

연세대학교
YONSEI UNIVERSITY

2012;149:1060-72.

10. Yang WS, Stockwell BR. Ferroptosis: death by lipid peroxidation. Trends in cell biology 2016;26:165-76.
11. Louandre C, Ezzoukhry Z, Godin C, Barbare JC, Mazière JC, Chauffert B, Galmiche A. Iron-dependent cell death of hepatocellular carcinoma cells exposed to sorafenib. International journal of cancer 2013;133:1732-42.
12. Dixon SJ, Stockwell BR. The role of iron and reactive oxygen species in cell death. Nature chemical biology 2014;10:9-17.
13. Gaschler MM, Stockwell BR. Lipid peroxidation in cell death. Biochemical and biophysical research communications 2017;482:419-25.
14. Martin-Sanchez D, Ruiz-Andres O, Poveda J, Carrasco S, Cannata-Ortiz P, Sanchez-Niño MD, et al. Ferroptosis, but not necroptosis, is important in nephrotoxic folic acid–induced AKI. Journal of the American Society of Nephrology: JASN 2017;28:218.
15. Linkermann A, Skouta R, Himmerkus N, Mulay SR, Dewitz C, De Zen F, et al. Synchronized renal tubular cell death involves ferroptosis. Proceedings of the National Academy of Sciences 2014;111:16836-41.
16. Friedmann Angeli JP, Schneider M, Proneth B, Tyurina YY, Tyurin VA, Hammond VJ, et al. Inactivation of the ferroptosis regulator Gpx4 triggers acute renal failure in mice. Nature cell biology 2014;16:1180-91.
17. Jang HR. Animal Models for Acute Kidney Injury. The Journal of the Korean Society for Transplantation 2017;31:111-6.
18. Li C, Jackson RM. Reactive species mechanisms of cellular hypoxia-reoxygenation injury. American Journal of Physiology-Cell Physiology 2002;282:C227-C41.
19. van Golen RF, Reiniers MJ, Vrisekoop N, Zuurbier CJ, Olthof PB, van Rheenen J, et al. The mechanisms and physiological relevance of glycocalyx degradation in hepatic ischemia/reperfusion injury. Antioxidants & redox signaling

연세대학교
YONSEI UNIVERSITY

2014;21:1098-118.

20. Ivanovic Z. Stem cell evolutionary paradigm and cell engineering. Transfusion Clinique et Biologique 2017;24:251-5.
21. Wong H-S, Dighe PA, Mezera V, Monternier P-A, Brand MD. Production of superoxide and hydrogen peroxide from specific mitochondrial sites under different bioenergetic conditions. Journal of Biological Chemistry 2017;292:16804-9.
22. Liaudet L, Szabó G, Szabó C. Oxidative stress and regional ischemia-reperfusion injury: the peroxynitrite–poly (ADP-ribose) polymerase connection. Coronary artery disease 2003;14:115-22.
23. Szabó G, Soós P, Bährle S, Zsengellér Z, Flechtenmacher C, Hagl S, Szabó C. Role of poly (ADP-ribose) polymerase activation in the pathogenesis of cardiopulmonary dysfunction in a canine model of cardiopulmonary bypass. European journal of cardio-thoracic surgery 2004;25:825-32.
24. Leaf DE, Rajapurkar M, Lele SS, Mukhopadhyay B, Boerger EA, Mc Causland FR, et al. Iron, hepcidin, and death in human AKI. Journal of the American Society of Nephrology: JASN 2019;30:493.
25. Gladwin MT, Kanias T, Kim-Shapiro DB. Hemolysis and cell-free hemoglobin drive an intrinsic mechanism for human disease. The Journal of clinical investigation 2012;122:1205-8.
26. Balla G, Jacob H, Eaton J, Belcher J, Vercellotti G. Hemin: a possible physiological mediator of low density lipoprotein oxidation and endothelial injury. Arteriosclerosis and thrombosis: a journal of vascular biology 1991;11:1700-11.
27. Jeney V, Balla J, Yachie A, Varga Z, Vercellotti GM, Eaton JW, Balla Gr. Pro-oxidant and cytotoxic effects of circulating heme. Blood, The Journal of the American Society of Hematology 2002;100:879-87.
28. Nagy E, Eaton JW, Jeney V, Soares MP, Varga Z, Galajda Z, et al. Red cells, hemoglobin, heme, iron, and atherogenesis. Arteriosclerosis, thrombosis, and

연세대학교
YONSEI UNIVERSITY

vascular biology 2010;30:1347-53.

29. Kristiansen M, Graversen JH, Jacobsen C, Sonne O, Hoffman H-J, Law SA, Moestrup SK. Identification of the haemoglobin scavenger receptor. Nature 2001;409:198-201.

30. Schaer DJ, Buehler PW, Alayash AI, Belcher JD, Vercellotti GM. Hemolysis and free hemoglobin revisited: exploring hemoglobin and hemin scavengers as a novel class of therapeutic proteins. Blood, The Journal of the American Society of Hematology 2013;121:1276-84.

31. Boretti FS, Buehler PW, D'Agnillo F, Kluge K, Glaus T, Butt OI, et al. Sequestration of extracellular hemoglobin within a haptoglobin complex decreases its hypertensive and oxidative effects in dogs and guinea pigs. The Journal of clinical investigation 2009;119:2271-80.

32. Cooper CE, Schaer DJ, Buehler PW, Wilson MT, Reeder BJ, Silkstone G, et al. Haptoglobin binding stabilizes hemoglobin ferryl iron and the globin radical on tyrosine β145. Antioxidants & redox signaling 2013;18:2264-73.

33. Banerjee S, Jia Y, Siburt CJP, Abraham B, Wood F, Bonaventura C, et al. Haptoglobin alters oxygenation and oxidation of hemoglobin and decreases propagation of peroxide-induced oxidative reactions. Free Radical Biology and Medicine 2012;53:1317-26.

34. Figueiredo RT, Fernandez PL, Mourao-Sa DS, Porto BN, Dutra FF, Alves LS, et al. Characterization of heme as activator of Toll-like receptor 4. Journal of Biological Chemistry 2007;282:20221-9.

35. Miller YI, Smith A, Morgan WT, Shaklai N. Role of hemopexin in protection of low-density lipoprotein against hemoglobin-induced oxidation. Biochemistry 1996;35:13112-7.

36. Gutteridge J, Smith A. Antioxidant protection by haemopexin of haem-stimulated lipid peroxidation. Biochemical Journal 1988;256:861-5.

37. Vinchi F, Gastaldi S, Silengo L, Altruda F, Tolosano E. Hemopexin prevents

연세대학교
YONSEI UNIVERSITY

endothelial damage and liver congestion in a mouse model of heme overload. The American journal of pathology 2008;173:289-99.

38. Tolosano E, Hirsch E, Patrucco E, Camaschella C, Navone R, Silengo L, Altruda F. Defective recovery and severe renal damage after acute hemolysis in hemopexin-deficient mice. Blood, The Journal of the American Society of Hematology 1999;94:3906-14.

39. Jiang C, Zhu W, Yan X, Shao Q, Xu B, Zhang M, Gong R. Rescue therapy with Tanshinone IIA hinders transition of acute kidney injury to chronic kidney disease via targeting GSK3β. Scientific reports 2016;6:36698.

40. Si J, Ge Y, Zhuang S, Wang LJ, Chen S, Gong R. Adrenocorticotropic hormone ameliorates acute kidney injury by steroidogenic-dependent and-independent mechanisms. Kidney international 2013;83:635-46.

41. Kang S-W, Adler SG, LaPage J, Natarajan R. p38 MAPK and MAPK kinase 3/6 mRNA and activities are increased in early diabetic glomeruli. Kidney international 2001;60:543-52.

42. Chavez R, Fraser DJ, Bowen T, Jenkins RH, Nesargikar P, Pino-Chavez G, Khalid U. Kidney ischaemia reperfusion injury in the rat: the EGTI scoring system as a valid and reliable tool for histological assessment. Journal of Histology and Histopathology 2016;3.

43. Park M, Kwon CH, Ha HK, Han M, Song SH. RNA-Seq identifies condition-specific biological signatures of ischemia-reperfusion injury in the human kidney. BMC nephrology 2020;21:1-12.

44. Nieuwenhuijs-Moeke GJ, Pischke SE, Berger SP, Sanders JSF, Pol RA, Struys MM, et al. Ischemia and reperfusion injury in kidney transplantation: relevant mechanisms in injury and repair. Journal of clinical medicine 2020;9:253.

연세대학교
YONSEI UNIVERSITY

ABSTRACT (IN KOREAN)

허혈-재관류 급성 신손상에서 haptoglobin과 hemopexin의 ferroptosis 억제에 의한 신보호 효과

<지도교수 유 태 현>

연세대학교 대학원 의학과

고 예 은

배경: 최근 연구에서 패혈증 및 심장 수술 후 환자의 경우 세포 외 헤모글로빈 농도가 증가하며, 이로 인해 급성 신부전을 유발할 수 있다는 것이 밝혀진 바가 있다. 세포 외 헤모글로빈에는 촉매 활성 철이 포함되어 있어 철 의존적 세포사, ferroptosis가 급성 신손상을 유발할 수 있다. 본 연구는 세포 외 헤모글로빈을 붙잡는 haptoglobin 및 hemopexin의 신장 보호 효과를 ferroptosis와 연관지어 동물 허혈-재관류 급성 신손상 모델을 이용하여 검증하고자 하였다.

방법: 허혈-재관류 신손상 동물 모델에서 2, 4, 6, 8 및 24 시간 후 세포 외 헤모글로빈 및 헤민 농도를 대조군과 허혈-재관류 신손상군 모두에서 평가하였다. 또한 허혈-재관류 신손상 모델에서 수술 30분 후 꼬리 정맥 주사를 통해 다양한 용량 (100, 200 mg/kg)의 haptoglobin 또는 hemopexin을 투여하였다. 세포 외 헤모글로빈, 헤민 및 신장 손상 표지자, 산화 스트레스 표지자 및 ferroptosis 표지자는 24시간 후에 평가하였다. 또한, 신장 손상 점수는 세포 사멸, 브러시 보더 상실, 캐스트 생성 및 세뇨관 확장의 비율을 기반으로 신장 조직에서 평가하였다. 정량적인 중합 효소 연쇄 반응, 웨스턴 블롯 분석 및 면역 조직 화학 염색을 ferroptosis와 관련된 기전을 평가하기 위해 수행하였다.

연세대학교
YONSEI UNIVERSITY

결과: 본 연구에서는 허혈-재관류 신손상군에서 시간이 경과함에 따라 세포 외 헤모글로빈 및 헤민 수준이 대조군과 비교하여 증가하였음을 확인하였다. Haptoglobin 주사는 용량과 관계없이 세포 외 헤모글로빈 수준을 감소시켰고, hemopexin 주사는 헤민 수준을 감소시켰다. 크레아티닌, BUN, NGAL 및 MDA 수준은 약제를 투여하지 않은 허혈-재관류 신손상군과 비교하였을 때 증가함을 확인하였다. 또한, haptoglobin 또는 hemopexin 치료는 약제를 투여하지 않은 허혈-재관류 신손상군과 비교하여 모든 용량에서 크레아티닌, BUN, MDA, NGAL 및 신장 손상 점수를 감소시켰다. 허혈-재관류 신손상군에서 시스틴/글루타메이트 반포터 시스템 Xc^- (*Slc7a11*)의 mRNA 발현은 대조군과 비교하여 감소하였으며, 페리틴 단백질 (ferritin heavy chain 1, *Fth1*) mRNA 발현은 증가하였다. 그러나 haptoglobin 또는 hemopexin 치료 시 *Slc7a11* mRNA 발현이 증가하고 *Fth1* 이 감소하는 결과를 확인하였다. 더불어, SLC7A11 및 GPX4에 대한 단백질 발현과 면역 조직화학 염색의 강도는 허혈-재관류 신손상군에서 감소하였으며, haptoglobin 또는 hemopexin 투여 후 개선되었다. 반면, FTH1은 반대의 경향을 보였다.

결론: 본 저자는 향후 포촉제 단백질인 haptoglobin 및 hemopexin이 ferroptosis를 억제함으로써 허혈-재관류 신손상의 예방제로서 도움이 될 수 있을 것으로 기대한다.

핵심되는 말: 급성 신손상, 허혈-재관류 손상, haptoglobin, hemopexin, 신보호